Journal of Biomechanics 87 (2019) 183–188

Contents lists available at ScienceDirect

Journal of Biomechanics

journal homepage: www.elsevier.com/locate/jbiomech
www.JBiomech.com

Short communication

An application of scissored-pair control moment gyroscopes in a design of wearable balance assistance device for the elderly

Parineak Romtrairat, Chanyaphan Virulsri *, Pairat Tangpornprasert

Center of Excellence for Prosthetic and Orthopedic Implant, Biomedical Engineering Research Center, Department of Mechanical Engineering, Faculty of Engineering, Chulalongkorn University, Phayathai Road, Pathumwan, Bangkok 10330, Thailand

ARTICLE INFO

Article history:
Accepted 8 March 2019

Keywords:
Balance assistance device
Sway fall
Limit of stability
Control moment gyroscopes

ABSTRACT

Impaired balance control ability and degraded functional mobility increases the risk of falling in elderly people. The elderly show more postural sway when standing compared with young people. A sway fall occurs when the center of gravity moves outside the limit of stability. In order to reduce the fall risk from the excessive sway, this study presents the design of wearable balance assistance device for the elderly. Scissored-pair control moment gyroscopes were selected as a torque actuator. A two-axis inclination sensor was used to detect the inclined angle of the wearer's body. The direction of sway was calculated from the detected inclined angle. The designed device weighs 8.2 kg with a height of 32 cm × width of 40 cm × depth of 22 cm. A multi-segment model of a standing human was used to investigate the device's performance for balance recovery. According to the simulations, balance recovery in any direction was successfully accomplished with the appropriate initial angle. The relationship between the effective initial angle and detected inclined angle was subsequently established. The stability provided by activation of the device was able to limit the unstable user's sway boundary. The designed device shows promise for use as a balance assistance device for the elderly.

1. Introduction

Accidental falls are major health problems for the elderly (Stenhagen et al., 2014). An individual's fall risk increases overtime with age when balance control ability and functional mobility degrade (Bronstein et al., 2004; Lord et al., 2007). The elderly show more postural sway when standing compared with young people (Hill et al., 2018; Roman-Liu, 2018). Sway-related falls tend to occur when the center of mass (COM) moves outside the limits of stability (LOS) which is smaller than the anthropometrical base of support (BOS) (Forth et al., 2011; Hof et al., 2005; Honarvar and Nakashima, 2014; Winter, 1995).

Recently, the concept of integrating a control moment gyroscope (CMG) into a wearable device for balance assistance was introduced. A 10-kg corset consisting of a single CMG was produced in the work of Lemus et al (Lemus et al., 2017). This single CMG design gave approximately 45 Nm torque in the allocated direction. In the work of Chiu and Goswami (Chiu and Goswami, 2014), two CMGs arranged as a scissored-pair were presented. This design weighs 7.7 kg and gives a maximum torque output of 20 Nm. However, to date, an analysis of applying the aforementioned wearable devices on human has not been examined. Plus, the method for detecting the direction of sway, the essential function of the device, has not been presented.

In order to reduce fall risk of the elderly from excessive sway in any direction, this study presents the design of a wearable balance assistance device. The selected actuator is a pair of scissored-pair control moment gyroscopes. The two-axis inclination sensor is integrated into the device to enable detection of sway direction. The application of the device was investigated by simulating the working device on a multi-segment human model. The details of generated torque calculations, the working mechanism, the method for detection and calculation of sway direction, and simulation with a human model are also elaborated.

2. Models and methods

2.1. The design of the SPCMGs balance assistance device

The scissored-pair control moment gyroscopes (SPCMGs) are a momentum exchange device acting as a torque actuator. The device consists of two similar CMGs with parallel gimbal axes. At the home position, the two CMGs are spinning at the similar speed

* Corresponding author.
E-mail address: chanyaphan.v@eng.chula.ac.th (C. Virulsri).

https://doi.org/10.1016/j.jbiomech.2019.03.015
0021-9290/

but in the opposite directions as shown in Fig. 1(a). The device generates torque $\vec{\tau}_g$ by precessing the spinning inertia with angular momentum $\vec{h}_r$ at the certain precession rate $\dot{\phi}$ (Brown, 2008; Chiu and Goswami, 2014). By counter-precessing the two CMGs simultaneously, the generated torques from both CMGs add up in the desired direction and cancel out the undesirable off-axis torque as shown in Fig. 1(b). The calculation of the generated torque summation is shown in Eq. (1).

$$\begin{aligned} \vec{\tau}_g &= -\dot{\phi} \times \vec{h}_r \\ \Sigma\vec{\tau} &= \vec{\tau}_{g1} + \vec{\tau}_{g2} \\ \| \Sigma\vec{\tau} \| &= 2h_r\dot{\phi}\cos\phi \end{aligned} \tag{1}$$

the time integral of the torque summation results in a change of angular momentum of the body ΔH_b which the device is attached to (Moon, 1998);

$$\Delta H_b = \int \Sigma\tau dt \tag{2}$$

combining Eqs. (1) and (2) yields,

$$\Delta H_b = \int 2h_r\dot{\phi}\cos\phi \; dt \tag{3}$$

according to the chain rule,

$$\dot{\phi}dt = d\phi \tag{4}$$

combining Eqs. (3) and (4) yields,

$$\Delta H_b = \int 2h_r\cos\phi \; d\phi \tag{5}$$

Eq. (5) shows that the magnitude of time integral of the torque summation depends on the sweeping precession angle. Due to the reciprocal characteristic of the generated torque, the beneficial range of precession starts from the initial state and stops at 90° incrementally. This gives,

$$\begin{aligned} \Delta H_b &= 2h_r \int_0^{\pi/2} \cos\phi \; d\phi \\ \Delta H_b &= 2h_r \end{aligned} \tag{6}$$

Eq. (6) shows the exchange of angular momentum from the device to the wearer's body. The angular momentum of spinning inertia plays an important role in the device's performance for balance recovery. To maximize the angular momentum and minimize the mass of the device, the maximum allowable spinning speed of the spinning disc and its diameter must be determined. To find the capability of the selected motors, the prototype of the designed device was made. At a limited operating current, the maximum possible spinning speed is 6000 rpm. The maximum possible precession rate was also assigned so that a 90° precession is accomplished in 0.5 s. The device's width shall not exceed 400 mm, which is the 95th percentile of a typical male's hip breadth (Pheasant and Haslegrave, 2006). With this contraint, two 186-mm-diameter aluminium discs are assigned to each gyroscope.

A two-axis inclination sensor is attached to the main body of the device. The inclined angles about the x-axis and y-axis are measured as $Inclined_x$ and $Inclined_y$ respectively. The sway direction ($\vec{s}_w$) and sway angle (β) are calculated from the two detected inclined angles as shown in Eq. (7). The gyroscopes are parallel-precessed to an initial angle (α) in order to align their angular momentum to the detected sway direction without generating torque as shown in Fig. 1(c). When the sway reaches a certain limit, the gyroscopes are counter-precessed in order to generate the assistance torque as shown in Fig. 1(d). The design of the SPCMGs balance assistance device is shown in Fig. 2. The size of the device's bounding box is H32cm × W40cm × D22cm. Its overall estimated weight is 8.2 kg excluding battery and controller units. The mass of the device's elements is shown in the appendix.

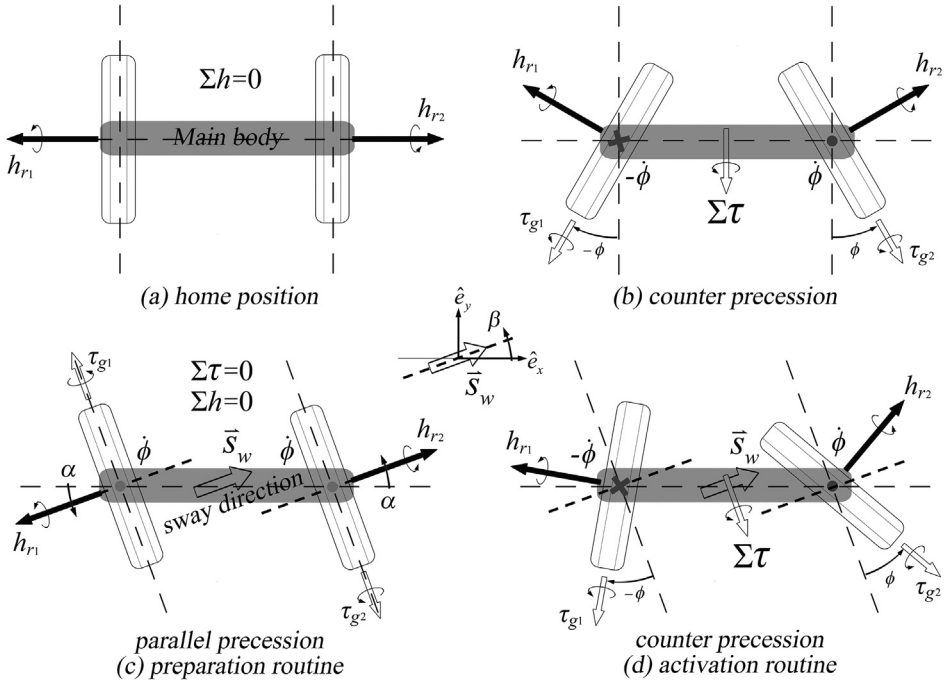

Fig. 1. A model and working principle of the scissored-pair control moment gyroscopes. (a) At home position, the summation of angular momentum of the system equals zero. (b) The summation of the two generated torques from counter precession of the CMGs is perpendicular to the direction of angular momentum at the initial state. (c) When sway occurs, the sway direction $\vec{s}_w$ is detected. The preparation routine starts. Both CMGs are parallel precessed to initial angle α. The resultant torque equals zero. (d) When an activation routine starts, the counter precession generates torque to recover balance.

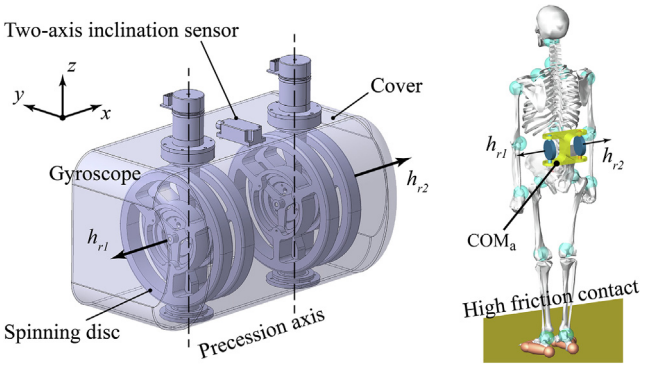

Fig. 2. Design of the SPCMG balance assistance device attached to the multi-segment human model. The device consists of two precessable gyroscopes for torque actuation and a two-axis inclination sensor to detect sway direction.

$$\overrightarrow{s}_w = Inclined_y\hat{e}_x - Inclined_x\hat{e}_y$$
$$\beta = tan^{-1}\left(-\frac{Inclined_x}{Inclined_y}\right) \quad (7)$$

2.2. A multi-segment model of a standing human for balance analysis

In the present study, a multi-segment human model in the biomechanical simulation software LifeMOD-BodySIM 2007.0.0 was used. The male model of 1.78 m in height and 77 kg in weight was generated using anthropometric data from a software library. The model consists of 19 segments and 18 joints (Ma et al., 2015). For a substitution of muscle modelling, passive stiffness of the lower extremity joints was assigned with a specified value (Lark et al., 2003; Silder et al., 2007). To avoid slipping fall and focus on sway fall, the friction of the contact between the floor and the model's feet is set to be very high. The model of the designed SPCMGs balance assistance device is fixed with the human model's central torso as shown in Fig. 2.

Nine directions of sway falls were simulated as shown in Fig. 3 (a). The direction starts varying from posterior (Path 1), rotates counter-clockwise to simulate right-sided lateral directions (Path 2–8), and continues varying until the direction reaches anterior (Path 9). The average COM positions of the human model and the designed device (COM_a) were studied in a simulation of balance recovery. The simulations start from rest at varied COM_a locations. The inclined angle of the device's body is recorded for the calculation of sway direction. A balance recovery is considered successful when the torque generated from the designed device is able to bring the COM_a back to its position while standing still (P0).

The simulations are divided into two experiments. In the first experiment, the two selected points of COM_a positioned along the latero-posterior fall on Path 4 were determined. The spinning speed was set at 6000 rpm. The initial angle (α) was varied in order to investigate which assigned initial angle yields successful balance recovery. In the second experiment, various points along the nine paths of sway fall were determined in order to depict the established limit of stability due to an activation of the device. All simulations were performed at a rate of 250 steps per second.

3. Results and discussion

3.1. Verification of an assigned initial angle for successful balance recovery

The first simulation started at the point P4.1 which was located on the latero-posterior sway fall Path 4. The body inclination angles about the x-axis and y-axis were 1.4° and 1.7° respectively. The calculated sway direction (β) was −40°. Activating the gyroscopes at an equal initial angle ($\alpha = -40°$) caused the model to fall anteriorly resulting in failed balance recovery. More lateral torque was needed, the smaller the initial angle was assigned. With a −20° initial angle, the movement of COM_a passed the point P0 exactly, as shown in Fig. 3(b). This satisfied the successful balance recovery requirement in this study. The second simulation started at point P4.2. The initial assigned angle varied incrementally by 1° yet COM_a movements did not pass P0 due to the activation of the device, as shown in Fig. 3(c). The simulation was considered failed in terms of balance recovery.

3.2. Verification of a balance recovery in any direction of sway fall

A total of 31 points along the nine paths of sway fall were determined in this study. The details are shown in Fig. 3(d) and Table 1. The LOS was established from the set of points (green dashed line) that yielded successful balance recovery by activation of the device. The sway boundary of an elderly person (brown dashed line) was drawn using the anterior/posterior and medial/lateral sway ranges of typical elderly people following Roman-Liu (Roman-Liu, 2018). In the worst-case scenario, the person's sway boundary was close to the posterior zone of functional stability limits (heel contact). This area yielded a very high risk of falling (Hernandez et al., 2012). The established LOS sufficiently covered the sway boundary and the hazardous posterior zone. As a result, the designed wearable balance assistance device was able to generate sufficient torque to overcome the excessive sway of the elderly.

Table 1 shows the differences between the calculated sway direction from Eq. (7) and the initial angle succeeding balance recovery. In every slant sway fall, the magnitude of the successful initial angle (α_s) was a diminishing value from the sway angle (β). The two-legged modelling used in this study revealed this finding. The equation for calculating an effective initial angle (α_{eff}) was established. When the correlation factor (k) is added to the Eq. (7), it yields Eq. (8). The value of k = 0.468 was obtained by averaging the proportion between the successful initial angle and the measured inclined angles ($Inclined_x$ and $Inclined_y$). The effective initial angle was calculated and shown in Table 1.

$$\alpha_{eff} = tan^{-1}\left(-k\frac{Inclined_x}{Inclined_y}\right) \quad (8)$$

In a practical use, the device shall be firmly fastened to the wearer's body in order to create a consistent link for torque transmission. However, the relative motion between the device and the wearer's body still occurs due to the wearer's movements; e.g. walking, and turning. The wearer's movements and the relative motion alter the measured inclined angles of the body. Consequently, it causes an uncertainty in the calculation of the effective initial angle. A capability of the two-axis inclination sensor to provide an accurate detection of sway direction in real-world situations needs a further investigation. An additional sensor for sway detection shall be determined for an improvement.

The safe weight recommendation of a backpack load is 10–15% of body weight (Adeyemi et al., 2017). The 8.2-kilogram device does not exceed the recommended weight but adding the backpack-load induces postural sway (Rugelj and Sevsek, 2011). In order to maintain the device's performance in torque generation, angular momentum from spinning gyroscopes needs to be preserved. Increased spinning speed is required if the size or the mass of the discs is reduced. The mechanical parts must be precisely manufactured and assembled in order to increase the operating spinning speed. Moreover, the control system for the device has to be well-developed because the fall risk occasionally comes from the assistive device itself (Bateni and Maki, 2005). The complete

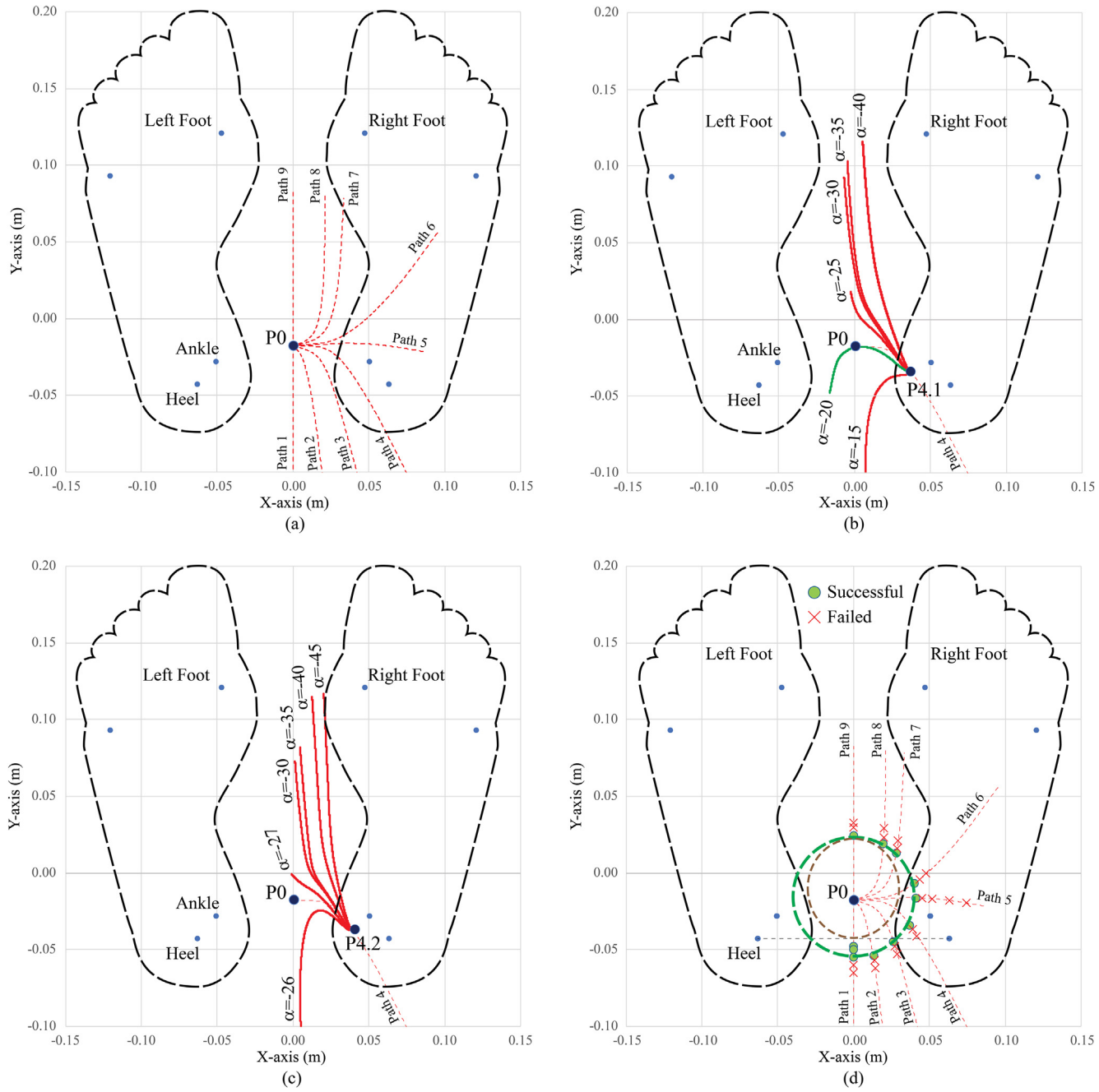

Fig. 3. The movements of average center of mass in balance recovery simulation. (a) The simulated sway falls in nine directions. Path 1 is a set of COM_a movements along the posterior sway fall. Paths 2 to 8 are sets of COM_a movements along the right-sided lateral sway fall. Path 9 is a set of COM_a movements along the anterior sway fall. The point P0 is the location of COM_a while the model is standing still. (b) The movement of COM_a due to different initial angles (α). The simulation starts at point P4.1. With an initial angle of −20°, the movement of COM_a passes the point P0. (c) The simulation starts at point P4.2. No COM_a movements passed P0. (d) The overall results of balance recovery simulation. The LOS of the designed device for the passive model of a standing human is drawn based on balance recovery results (green dashed line). The sway boundary of an elderly person (brown dashed line) after Roman-Liu (Roman-Liu, 2018) is drawn for comparison. (For interpretation of the references to colour in this figure legend, the reader is referred to the web version of this article.)

prototype of the designed device will be produced and its performance will be tested in a future study.

4. Conclusion

In this study, the principle showing how torque can be generated by SPCMGs in the assigned direction was investigated. The wearable SPCMG balance assistance device was designed for this purpose. Using a simulation with a multi-segment model of a standing human, balance recovery in any direction was successfully accomplished with the appropriate initial angle. The relationship between the effective initial angle and detected inclined angle was subsequently established. This finding can improve the performance of the designed wearable balance assistance device. The device was shown to be able to generate sufficient torque against the excessive sway of a typical elderly user. The designed balance assistance device using SPCMG technology was able to generate sufficient torque for balance recovery against sway fall in any direction on a transverse plane.

Table 1
Overall results of balance recovery simulation.

Point	Path	Inclined angle		Balance Recovery	Sway direction		Successful initial angle			α_{eff} (deg)
		x (deg)	y (deg)		$\vec{s}_w$	β (deg)	$\vec{h}_{r1}$	$\vec{h}_{r2}$	α_s (deg)	
P1.1	Path 1	2.9	0.0	Successful	↓	-90	↑	↓	-90	-90
P1.2	Path 1	3.1	0.0	Successful	↓	-90	↑	↓	-90	-90
P1.3	Path 1	3.5	0.0	Successful	↓	-90	↑	↓	-90	-90
P1.4	Path 1	4.0	0.0	Failed	↓	-90	-	-	-	-
P1.5	Path 1	4.4	0.0	Failed	↓	-90	-	-	-	-
P2.1	Path 2	3.4	0.5	Successful	↘	-82	↖	↘	-69	-73
P2.2	Path 2	3.7	0.6	Failed	↓	-81	-	-	-	-
P2.3	Path 2	4.1	0.7	Failed	↓	-80	-	-	-	-
P3.1	Path 3	2.5	1.1	Successful	↘	-67	↖	↘	-50	-47
P3.2	Path 3	2.8	1.2	Failed	↘	-67	-	-	-	-
P3.3	Path 3	3.3	1.3	Failed	↘	-68	-	-	-	-
P4.1	Path 4	1.4	1.7	Successful	↘	-40	←	→	-20	-22
P4.2	Path 4	1.7	1.7	Failed	↘	-45	-	-	-	-
P4.3	Path 4	2.0	1.8	Failed	↘	-48	-	-	-	-
P5.1	Path 5	0.2	1.9	Successful	→	-6	←	→	0	-3
P5.2	Path 5	0.2	2.0	Failed	→	-6	-	-	-	-
P5.3	Path 5	0.2	2.3	Failed	→	-5	-	-	-	-
P5.4	Path 5	0.2	2.7	Failed	→	-4	-	-	-	-
P5.5	Path 5	0.2	3.1	Failed	→	-4	-	-	-	-
P6.1	Path 6	-1.1	1.9	Successful	↗	30	←	→	15	15
P6.2	Path 6	-1.4	2.1	Failed	↗	34	-	-	-	-
P6.3	Path 6	-1.7	2.3	Failed	↗	36	-	-	-	-
P7.1	Path 7	-2.8	1.5	Successful	↗	62	↙	↗	38	41
P7.2	Path 7	-3.1	1.5	Failed	↗	64	-	-	-	-
P7.3	Path 7	-3.6	1.5	Failed	↗	67	-	-	-	-
P8.1	Path 8	-3.3	1.1	Successful	↗	72	↙	↗	62	56
P8.2	Path 8	-3.8	1.1	Failed	↗	74	-	-	-	-
P8.3	Path 8	-4.3	1.1	Failed	↗	76	-	-	-	-
P9.1	Path 9	-3.7	0.0	Successful	↑	90	↓	↑	90	90
P9.2	Path 9	-4.2	0.0	Failed	↑	90	-	-	-	-
P9.3	Path 9	-4.5	0.0	Failed	↑	90	-	-	-	-

Acknowledgements

The present study was supported by the Ratchadaphiseksomphot Endowment Fund of Chulalongkorn University (RES560530081-AS) and the 100th Anniversary Chulalongkorn University Fund for Doctoral Scholarship.

Conflict of interest

There is no conflict of interest. The authors are responsible for the content and writing of this article. This study was supported by the Ratchadaphiseksomphot Endowment Fund of Chulalongkorn University and the 100th Anniversary Chulalongkorn University Fund for Doctoral Scholarship. There is no any other organizations who supported this study.

Appendix A. Supplementary material

Supplementary data to this article can be found online at https://doi.org/10.1016/j.jbiomech.2019.03.015.

References

Adeyemi, A.J., Rohani, J.M., Rani, M.R.A., 2017. Backpack-back pain complexity and the need for multifactorial safe weight recommendation. Appl. Ergon. 58, 573–582.

Bateni, H., Maki, B.E., 2005. Assistive devices for balance and mobility: benefits, demands, and adverse consequences. Arch. Phys. Med. Rehab. 86, 134–145.

Bronstein, A.M., Brandt, T., Woollacott, M.H., Nutt, J.G., 2004. Clinical disorders of balance, posture and gait, 2nd ed., Arnold.

Brown, D. Control moment gyros as space-robotics actuator. AIAA Guidance, Navigation, and Control Conference and Exhibition; 2008.

Chiu, J., Goswami, A. Design of a wearable scissored-pair control moment gyroscope (SP-CMG) for human balance assist. In: Proceedings of the ASME 2014 international design engineering technical conferences & computers and information in engineering conference.

Forth, K.E., Fiedler, M.J., Paloski, W.H., 2011. Estimating functional stability boundaries for bipedal stance. Gait Posture 33, 715–717.

Hernandez, M.E., Ashton-Miller, J.A., Alexander, N.B., 2012. Age-related changes in speed and accuracy during rapid targeted center of pressure movements near the posterior limit of the base of support. Clin. Biomech. 27, 910–916.

Hill, M.W., Duncan, M.J., Oxford, S.W., Kay, A.D., Price, M.J., 2018. Effects of extern al loads on postural sway during quiet stance in adults aged 20–80 years. Appl. Ergon. 66, 64–69.

Hof, A.L., Gazendam, M.G.J., Sinke, W.E., 2005. The condition for dynamic stability. J. Biomech. 38, 1–8.

Honarvar, M.H., Nakashima, M., 2014. A new measure for upright stability. J. Biomech. 47, 560–567.

Lark, S.D., Buckley, J.G., Bennett, S., Jones, D., Sargeant, A.J., 2003. Joint torques and dynamic joint stiffness in elderly and young men during stepping down. Clin. Biomech. 18, 848–855.

Lemus, D., van Frankenhuyzen, J., Vallery, H., 2017. Design and evaluation of a balance assistance control moment gyroscope. J. Mech. Robot.

Lord, S., Sherrington, C., Menz H., Close, J., 2007. Falls in Older People: Risk Factors and Strategies for Prevention. 2nd ed. Cambridge.

Ma, J., Kharboutly, H., Benali, A., Benamar, F., Bouzit, M., 2015. Joint angle estimation with accelerometers for dynamic postural analysis. J. Biomech. 48, 3616–3624.

Moon, F.C., 1998. Applied Dynamics: With Applications to Multibody and Mechatronics System. John Wiley & Sons.

Pheasant, S., Haslegrave, C., 2006. Bodyspace: Anthropometry, Ergonomics and the Design of Work. Taylor and Francis, Florida.

Roman-Liu, D., 2018. Age-related changes in the range and velocity of postural sway. Arch. Gerontol. Geriatr. 77, 68–80.

Rugelj, D., Sevsek, F., 2011. The effect of load mass and its placement on postural sway. Appl. Ergon. 42, 860–866.

Silder, A., Whittington, B., Heiderscheit, B., Thelen, D.G., 2007. Identification of passive elastic joint moment–angle relationships in the lower extremity. J. Biomech. 40, 2628–2635.

Stenhagen, M., Ekstrom, H., Nordell, E., Elmstahl, S., 2014. Accidental falls, health-related quality of life and life satisfaction: a prospective study of the general elderly population. Arch. Gerontol. Geriatr. 58, 95–100.

Winter, D.A., 1995. Human balance and posture control during standing and walking. Gait Posture 3, 193–214.